

EgoTV : Egocentric Task Verification from Natural Language Task Descriptions

Rishi Hazra^{1*}, Brian Chen², Akshara Rai², Nitin Kamra², Ruta Desai²✉

¹Örebro University ²Meta

rishi.hazra@oru.se, {bc2754, nitinkamra, akshararai, rutadesai}@meta.com

<https://rishi.hazra.github.io/EgoTV>

Abstract

To enable progress towards egocentric agents capable of understanding everyday tasks specified in natural language, we propose a benchmark and a synthetic dataset called Egocentric Task Verification (EgoTV). The goal in EgoTV is to verify the execution of tasks from egocentric videos based on the natural language description of these tasks. EgoTV contains pairs of videos and their task descriptions for multi-step tasks – these tasks contain multiple sub-task decompositions, state changes, object interactions, and sub-task ordering constraints. In addition, EgoTV also provides abstracted task descriptions that contain only partial details about ways to accomplish a task. Consequently, EgoTV requires causal, temporal, and compositional reasoning of video and language modalities, which is missing in existing datasets. We also find that existing vision-language models struggle at such all round reasoning needed for task verification in EgoTV. Inspired by the needs of EgoTV, we propose a novel Neuro-Symbolic Grounding (NSG) approach that leverages symbolic representations to capture the compositional and temporal structure of tasks. We demonstrate NSG’s capability towards task tracking and verification on our EgoTV dataset and a real-world dataset derived from CrossTask [82] (CTV). We open-source the EgoTV and CTV datasets and the NSG model for future research on egocentric assistive agents.

1. Introduction

Inspired by recent progress in visual systems [40, 65], we consider an assistive egocentric agent capable of reasoning about daily activities. When invoked via natural language commands, for e.g., while baking a cake, the agent understands the steps involved in baking, tracks progress through the various stages of the task, detects and proactively prevents mistakes by making suggestions. Such a vir-

tual agent [11] would empower users to learn new skills and accomplish tasks efficiently.

Developing this egocentric agent capable of tracking and verifying everyday tasks based on their natural language specification is challenging for multiple reasons. First, such an agent must reason about various ways of doing a *multi-step* task specified in natural language. This entails decomposing the task into relevant actions, state changes, object interactions as well as any necessary causal and temporal relationships between these entities. Secondly, the agent must ground these entities in egocentric observations to track progress and detect mistakes. Lastly, to truly be useful, such an agent must support tracking and verification for a combination of tasks and, ideally, even unseen tasks. These three challenges – causal and temporal reasoning about task structure from natural language, visual grounding of sub-tasks, and compositional generalization – form the core goals of our work.

As our first contribution, we propose a benchmark – *Egocentric Task Verification* (EgoTV ) – and a corresponding dataset in the AI2-THOR [29] simulator. Given a natural language (NL) task description and a corresponding egocentric video of an agent, the goal of EgoTV is to verify whether the task was successfully completed in the video or not. EgoTV contains multi-step tasks with *ordering* constraints on the steps and *abstracted* NL task descriptions with omitted low-level task details inspired by the needs of real-world assistants. We also provide splits of the dataset focused on different generalization aspects, e.g., unseen visual contexts, compositions of steps, and tasks (see Figure 1). Consequently, EgoTV dataset provides the fine-grained control necessary for rigorous testing and refinement of task reasoning models, which is often missing in real-world datasets [17, 10]. Yet, EgoTV mirrors the real world by leveraging visual photo-realism and task diversity.

Our second contribution is a novel approach for order-aware visual grounding – *Neuro-Symbolic Grounding* (NSG), capable of compositional reasoning and generalizing to unseen tasks owing to its ability to leverage ab-

*Work done while interning at Meta.

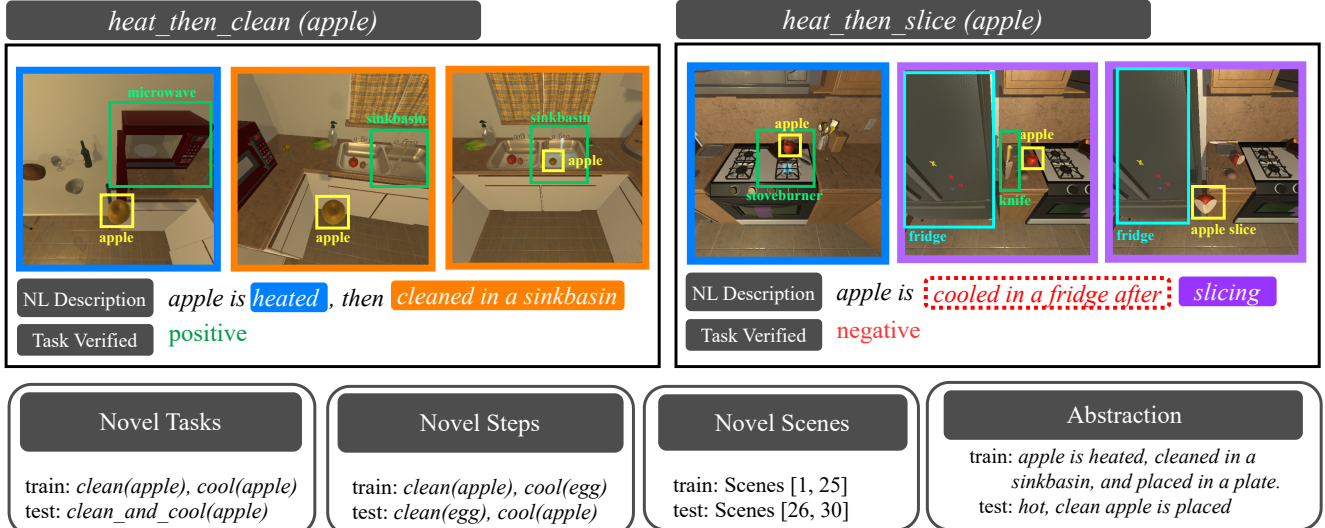


Figure 1. **EgoTV benchmark.** A positive example [Left] and a negative example [Right] from the train set along with illustrative examples from the test splits [Bottom] of EgoTV are shown. The test splits are focused on generalization to novel compositions of tasks, unseen sub-tasks or steps and scenes, and abstraction in NL task descriptions. The bounding boxes are solely for demonstration purposes and are not used during training/inference.

stract NL descriptions along with compositional and temporal structure of tasks (task decomposition, ordering). In contrast, state-of-the-art vision-language models [76, 50, 36, 3] struggle to ground NL descriptions in egocentric videos, and do not generalize to unseen tasks. NSG outperforms these models by **33.8%** on compositional generalization and **32.8%** on abstractly described task verification. Finally, to evaluate NSG on real-world data, we instantiate EgoTV on the CrossTask [82] instructional video dataset. We find that it also outperforms state-of-the-art models at task verification on CrossTask. We hope that the EgoTV benchmark and dataset will enable future research on egocentric agents capable of aiding in everyday tasks.

2. Related Work

Video-based Task Understanding. Understanding tasks from videos has been a long-standing theme in vision research with focus on recognizing activities [58, 10], human-object interactions [25, 17], and object state changes [60, 14] using egocentric or exocentric videos. But apart from recognizing actions, objects, and state changes, task verification also requires understanding temporal orderings between them. Our work is, therefore, closer to research on understanding instructional tasks [82, 62], which require reasoning about multiple, ordered steps. Prior works focus on either learning the order of steps [4, 37, 24, 42] or use step-ordering as a supervisory signal for learning step-representations or step-segmentation [82, 56]. Instead, we are focused on video-based order verification of steps described in NL, akin to [49].

Temporal Video Grounding. Our EgoTV benchmark is also closely related to the problem of Temporal Video Grounding (TVG) [43, 20, 52, 60]. However, prior work on TVG predominantly focuses on localizing a single action in the video [59, 27]. In contrast, EgoTV requires localizing multiple actions, wherein actions could have partial ordering, i.e., actions could have more than one valid ordering amongst them.

Vision-Language Benchmarks. Various benchmarks have been proposed for enabling models that can reason across video and language modalities (see Table 1). Examples include video question answering [74, 69, 18, 21, 68, 31, 63, 16], video-based entailment [38], and embodied task completion [57, 47, 61]. However, these benchmarks focus on individual specific aspects of multimodal reasoning, e.g., compositional reasoning (AGQA [18], ActivityNet-QA [21], TVQA [31], and CATER [16]) or causal reasoning (NExT-QA [69], CoPhy [5], Causal-VidQA [33], EgoTaskQA [26], and VIOLIN [38]). In comparison, EgoTV focuses on both causal and compositional reasoning and further requires visual grounding of both objects and actions from text, similar to STAR [68] and CLEVRER [74], albeit in egocentric settings. Unlike embodied task completion benchmarks whose objective is to develop robotic agents that can *perform everyday tasks* through task-planning (ALFRED [57], TEACH [47]) and control (Behavior [61]), EgoTV benchmark’s objective is to develop virtual agents that can *track and verify everyday tasks* performed by humans. Akin to NLP *Entailment* problem [9, 70], it can also be viewed as a video-based entailment problem – where a given “premise” (video) is val-

	Reasoning			Dataset Characteristics		
	compositional	causal	temporal	egocentric	real-world	diagnostic tools
CLEVRER [74]	✓	✓	✓	✗	✗	✓
Next-QA [69]	✗	✓	✓	✗	✓	✓
ActivityNet-QA [21]	✗	✗	✓	✗	✓	✗
STAR [68]	✓	✓	✓	✗	✓	✓
Causal-VidQA [33]	✗	✓	✗	✗	✓	✓
EPIC-KITCHENS [10]	✓	✓	✗	✓	✓	✓
Ego-4D [17]	✗	✓	✗	✓	✓	✓
VIOLIN [38]	✗	✓	✗	✗	✓	✗
Cross-Task [82]	✓	✓	✓	✗	✓	✗
EgoTV 	✓	✓	✓	✓	✗	✓

Table 1. **EgoTV vs. existing video-language datasets.** EgoTV benchmark enables systematic investigation (diagnostics) on compositional, causal (e.g., effect of actions), and temporal (e.g., action ordering) reasoning in egocentric settings. Table 5 in Appendix provides a more comprehensive comparison.

idated by a “hypothesis” (task description).

Vision-Language Models. Vision-Language Models (VLMs) [50, 36, 39, 32, 76] pre-trained on large-scale image-text or video-language narration pairs have demonstrated enhanced performance on certain compositional [34] and causal [60] tasks. However, they generally struggle to handle compositionality and order sensitivity [77, 64]. Instead, NSG explicitly targets order awareness and compositionality for generalization in task verification using neuro-symbolic reasoning.

Neuro-symbolic Models. Neuro-symbolic models combine feature extraction through deep learning with symbolic reasoning [54, 68] to capture compositional substructures. These models either reason on static images to recognize object attributes and relations (NS-CL [41], NS-VQA [75], CLOSURE [6], and ∇ -FOL [2]), or on videos to recognize spatio-temporal and causal relations (NS-DR [74] and DCL [8]). We extend this to tracking multi-step actions.

3. EgoTV Benchmark and Dataset

We present the *Egocentric Task Verification* (EgoTV) benchmark and dataset. To enable task tracking and verification for egocentric agents, EgoTV contains: 1) *multi-step* tasks with *ordering constraints* to capture the causal and temporal nature of everyday tasks, 2) *multimodality* – language in addition to the egocentric video to allow language-based human-agent interaction.

EgoTV also aims to enable the systematic study of generalization in task verification (see Table 1). To this end, we create the EgoTV dataset using a photo-realistic simulator AI2-THOR [29] – as a rich testbed for future research on generalizable agents for task tracking and verification. Our synthetic dataset serves as a valuable proxy of real-world performance of various task verification models while providing control over various factors affecting task reasoning.

Lastly, we also create a real-world task verification dataset (§ 4) using the CrossTask dataset [82]. While this dataset is not egocentric and is limited in its ability to systematically evaluate the generalization of task reasoning models, it enables the testing of task verification models in real world.

3.1. Definitions

Benchmark. The objective is to determine if a task described in natural language has been correctly executed by the agent in a given egocentric video.

Tasks. Each task in EgoTV consists of multiple *partially-ordered sub-tasks* or steps. A sub-task corresponds to a single object interaction via one of the six actions: *heat*, *clean*, *slice*, *cool*, *place*, *pick*, and is parameterized by a *target* object of interaction¹. By using the “actionable” properties of objects in AI2-THOR [29], we ensure that the sub-tasks are parameterized with appropriate target objects in EgoTV, e.g., *heat(book)* will never occur.

Real-world tasks consist of sub-tasks with ordering constraints, either due to physical restrictions (e.g., picking up a knife before slicing) or task semantics (e.g., slicing vegetables before frying). We allow EgoTV tasks to be partially ordered, with some steps following strict ordering, e.g. *pick* sub-task happens before *place* sub-task, while others are order-independent.

The ordering constraints between sub-tasks are captured in the task description using specifiers such as *and*, *then*, and *before/after*. For simplicity, we will refer to a task using $\langle \text{sub-task} \rangle - \langle \text{ordering-specifier} \rangle$ notation, irrespective of the actual task description. Such tasks can then be instantiated by specifying an (*object*) of interaction. An example task instance from EgoTV: *heat_then_clean(apple)* is shown in Fig. 1 with its NL description: “apple is heated,

¹Except the *place* sub-task, which is additionally parameterized by a *receptacle* object, we currently limit our EgoTV dataset to sub-tasks involving only a single target object.

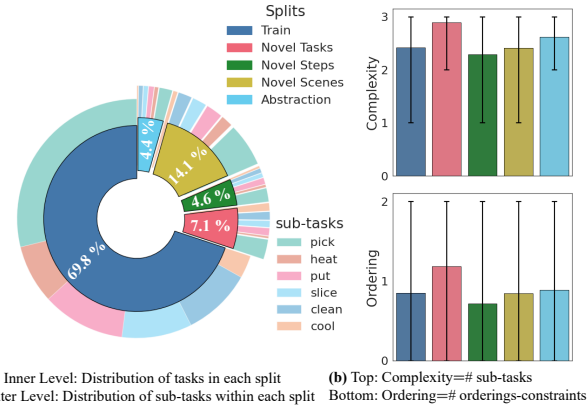


Figure 2. **EgoTV dataset.** Sub-tasks and tasks, including their difficulty measures (§ 3.2.2) are shown per split. Novel Scenes have more tasks since all the train tasks are repeated in unseen scenes. Likewise, complexity and ordering are higher in Novel Tasks due to the addition of unseen sub-tasks.

then cleaned in a sinkbasin”. The task consists of two ordered sub-tasks: *heat* \rightarrow *clean* on *target* object: apple. We adopt this terminology from ALFRED [57].

3.2. Dataset

As shown in Fig. 1, EgoTV dataset consists of (task description, video) pairs with positive or negative task verification labels. By combining the six sub-tasks *heat*, *clean*, *slice*, *cool*, *put*, *pick* with different ordering constraints, we create 82 tasks for EgoTV (see Appendix 8.3 for an exhaustive list). Tasks are instantiated with 130 target objects (excluding visual variations in shape, texture, and color) and 24 receptacle objects, totaling 1038 task-object combinations. These are performed in 30 different kitchen scenes. We also provide comprehensive annotations for each video, including frame-by-frame breakdowns for sub-tasks, object bounding boxes, and object state information (e.g., *hot*, *cold*, etc.) to facilitate future research.

3.2.1 Generation

Task-video Generation. We generate the videos in our dataset by leveraging the ALFRED setup [57]. ALFRED allows us to specify the EgoTV tasks using Planning Domain Definition Language (PDDL) and then to generate plans for achieving these tasks using the Metric-FF planner [23]. We execute these plans using the AI2-THOR simulator and obtain their corresponding videos. Further details on encoding tasks using PDDL and planning are in Appendix 8.1.

Task-description Generation. We convert the plans generated for each task into positive and negative task descriptions using templates. Appendix 8.2 provides details on the process and example templates.

3.2.2 Evaluation

Metrics. We use accuracy and F1 to measure the efficacy of models on EgoTV task verification benchmark. To capture the difficulty of tracking and verifying tasks, we introduce two measures: (1) *Complexity*: measuring the number of sub-tasks in a task, which impacts the video length and requires higher action and object grounding, and (2) *Ordering*: measuring the number of ordering constraints in a task and measures the difficulty of temporal reasoning required to track and verify tasks. We evaluate model scalability by testing on tasks with varying complexity and ordering.

Generalization. EgoTV dataset enables systematic exploration of generalization in task tracking and verification via four test splits that focus on generalization to novel steps, tasks, visual contexts/scenes, and abstract task descriptions.

- **Novel Tasks:** Unseen compositions of seen sub-tasks. For e.g., if train set is $\{\text{clean}(\text{apple}), \text{cool}(\text{apple})\}$, then this test split would contain tasks like: $\{\text{clean_and_cool}(\text{apple}), \text{clean_then_cool}(\text{apple}), \text{cool_then_clean}(\text{apple})\}$.
- **Novel Steps:** Unseen compositions of sub-task actions and target objects. For e.g., if the train set is $\{\text{clean}(\text{apple}), \text{cool}(\text{egg}), \text{clean_and_cool}(\text{tomato})\}$, then this test split would contain tasks like: $\{\text{clean}(\text{egg}), \text{cool}(\text{apple}), \text{clean_and_cool}(\text{apple})\}$.
- **Novel Scenes:** This test split contains the same tasks as in the train set. However, the tasks are executed in unseen kitchen scenes.
- **Abstraction:** Abstract task descriptions, which lack the low-level details of the task. For instance, for a *heat_and_clean(apple)* task, the full task description in the train set could be “apple is heated in a microwave and cleaned in sink basin”, while the abstract task description in this split could be “apple is heated and cleaned”.

Note that all the test splits and the train set are disjoint from each other. Novel Steps split tests an EgoTV model’s ability to understand generalizable object affordances and tool usage. For instance, once a model learns the *slice* action on an apple, this split tests if the model can apply it to an orange. On the other hand, the Novel Tasks split tests the generalization of a model’s temporal and causal reasoning capabilities on unseen compositions and orderings of known sub-tasks. Existing real-world datasets like Ego4D [17] and EPIC-KITCHENS [10] fail to provide such systematic control and precise diagnostics across various relevant yet independent factors affecting task reasoning.

3.2.3 Statistics

EgoTV dataset consists of 7,673 samples (train set: 5,363 and test set: 2,310). The split-wise division is Novel Tasks:

540, Novel Steps: 350, Novel Scenes: 1082, Abstraction: 338. The total duration of the egocentric videos in the EgoTV dataset is 168 hours, with an average video length of 84 seconds. To ensure diversity, each task in EgoTV is associated with ≈ 10 different task description templates (inclusive of positive and negative scenarios). We also keep an additional template set for the abstraction split. The task descriptions consist of 9 words on average, with a total vocabulary size of 72. On average, there are 4.6 sub-tasks per task in the EgoTV dataset, and each sub-task spans approximately 14 frames. Additionally, there are 2.4 ways to verify a task. This requires the virtual agent to understand all possible temporal orderings between sub-tasks from the task description for successful task verification. Real-world datasets mainly focus on recognizing actions, objects, and state changes [17, 10] without this ambiguity. Figure 2 shows a comparison of train and test splits (more analysis in Appendix 8.3).

4. CrossTask Verification (CTV) Dataset

Drawing from the EgoTV dataset, we introduce CrossTask Verification (CTV) dataset, using videos from the CrossTask dataset [82], to evaluate task verification models on real-world videos. In CTV, we prioritize assessing real-world performance of task verification models over systematic study of their generalization capabilities, unlike EgoTV. Thus, CTV complements EgoTV dataset – CTV and EgoTV together provide a solid test-bed for future research on task verification.

4.1. Dataset Generation

Like EgoTV, CTV consists of paired task descriptions and videos for task verification. CrossTask has 18 task classes, each with roughly 150 videos, from which we create $\approx 2.7K$ samples. We generate task descriptions by concatenating action step annotations in CrossTask. The model’s objective is to determine whether the action steps (sub-tasks) and their sequence in the video align with the description. See Appendix 9 for dataset construction details.

4.2. Evaluation

Metrics. Following EgoTV, we use accuracy and F1 to measure the efficacy of the models on the CTV dataset.

Generalization. We construct a test set using videos with seen action steps but in previously unseen compositions. To ensure novel compositions, we train on videos with up to 3 action steps and test on those with 4, as illustrated in Figure 3. While this mirrors the Novel Task split in EgoTV, the CTV test set also contains unseen visual contexts (videos) – a result of limited control during dataset creation.

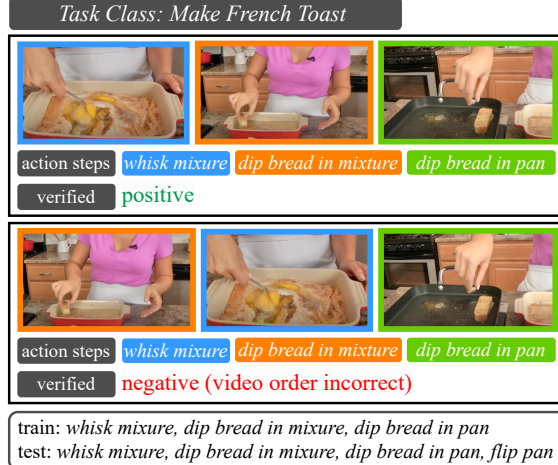


Figure 3. CrossTask Verification (CTV) dataset.

5. Neuro-Symbolic Grounding (NSG)

EgoTV requires visual grounding of task-relevant entities such as actions, state changes, etc. extracted from NL task descriptions for verifying tasks in videos. To enable grounding that generalizes to novel compositions of tasks and actions, we propose the Neuro-symbolic Grounding (NSG) approach. NSG consists of three modules: a) semantic parser, which converts task-relevant states from NL task descriptions into symbolic graphs, b) query encoders, which generate the probability of a node in the symbolic graph being grounded in a video segment, and c) video aligner, which uses the query encoders to align these symbolic graphs with videos. NSG thus uses intermediate symbolic representations between NL task descriptions and corresponding videos to achieve compositional generalization.

5.1. Queries for Symbolic Operations

To encode tasks, NSG captures task-relevant visual and relational information in a structured manner via symbolic operators called *queries*. For instance, the task description *heat an apple* can be symbolically captured by the query: *StateQuery(apple, hot)*. Similarly, the task description *place steak on grill* can be captured by *RelationQuery(steak, grill, on)*, which represents the relation (*on*) between objects *steak* and *grill*. Queries are characterized by *types* and *arguments* and are stored in a text format. Table 2 shows the various query types and their arguments. Different query types capture different aspects, e.g., attributes, relations, etc., thereby enabling a rich symbolic representation of everyday tasks.

5.2. Semantic Parser for Task Descriptions

The symbolic operators, i.e., queries, allow the semantic parser to represent a task’s partial-ordered steps using a symbolic graph. Specifically, the parser translates a NL task

Query Type	Signature	Semantics
StateQuery	(Object, State), Video $\mapsto \mathbb{P}$	Queries the state (hot, cold, clean, ripe) of object in a video and returns the probability of the object state being detected. Example instructions: <i>heat an apple, clean a spoon</i> .
RelationQuery	(Object, Object/Receptacle, Relation), Video $\mapsto \mathbb{P}$	Queries the relation between two objects or an object and a receptacle in a video and returns the probability of the relation being detected. Example instructions: <i>put apple in basket, place spoon to the left of plate</i> .
ActionQuery	(Subtask, *Objects, *Relation), Video $\mapsto \mathbb{P}$	Queries for a sub-task with one or more arguments (*) in a video and returns the probability of the sub-task being executed. Example instructions: <i>whisk mixture, pour lemonade into glass</i> .

Table 2. **NSG’s query types for task verification in EgoTV and CTV.** The query types `StateQuery` and `RelationQuery` are used in EgoTV, whereas `ActionQuery` is used in CrossTask. Each query type τ is modeled using a neural network f^{θ_τ} accepts unique arguments (a) and video frames (v) as input and generates an output probability $\mathbb{P} = f^{\theta_\tau}(a, v)$ of the *query* being true in the video v .

description into a graph $G(V, E)$, where a vertex $n_i \in V$ represents a query and an edge $e_{ij} : n_i \rightarrow n_j \in E$ is an ordering constraint indicating that n_i must precede n_j (Figure 4a). We experiment with two different methods to parse language descriptions of tasks to graphs – (i) finetuning language models and (ii) few-shot prompting of language models. For details, refer to Appendix 10.2. We perform a topological sort with the graph G and generate all the possible sequences of queries consistent with the sort. For example, the topological sorting of the graph in Figure 4(a) yields two ordered sequences: (n_0, n_1, n_2, n_3) , (n_0, n_2, n_1, n_3) . Note that this does not include all physically possible ways to complete a task, but a super-set of all possible sequences of task-relevant queries, including some infeasible sequences². However, this super-set is useful because a task can be verified as accomplished if any sequence in this set can be ascertained to occur in the video.

Notably, all EgoTV tasks map to acyclic graphs through temporal disambiguation. While this can support tasks with repeated actions, such as: (Task) *pick two apples*; (Graph) $\text{pick(apple)} \rightarrow \text{pick(apple)}$; tasks that require (recursively) repeating action sequences until a desired state is reached, might result in cyclic graphs. Examples include unstacking an arbitrary number of dishes or searching for an ingredient. While currently absent in EgoTV, extending to such tasks would be a valuable future direction.

5.3. Query Encoders for Grounding

Query Encoders are neural network modules that evaluate whether a query is satisfied in an input video. Specifically, a query encoder f^{θ_τ} for a query n of type τ (e.g., `StateQuery`, `RelationQuery` etc.), accepts NL arguments (a) corresponding to objects and relations in n and a video (v) to generate the probability $\mathbb{P} = f^{\theta_\tau}(a, v)$ of the desired query being true in the video. Learnable parameters

²For instance, in Figure 4a, n_1 and n_2 are at the same topological level, but the sub-task in query n_1 could invalidate pre-conditions for n_2 . Hence, a physically plausible task requires n_2 followed by n_1 and not vice versa. Note that EgoTV does not have physically implausible tasks.

corresponding to different query type encoders in an NSG model are jointly represented as $\theta = \bigcup_\tau \theta_\tau$.

Both the text arguments a of the query and the frames of the input video v are encoded using a pre-trained CLIP encoder [50]. The token-level and frame-level representations from CLIP are separately aggregated using two LSTMs [22] to obtain aggregated features for a and v , respectively. These features are then fused and passed through the neural network f^{θ_τ} to obtain the probability \mathbb{P} of the query being true in the video (see Figure 4a).

5.4. Video Aligner for Task Verification

This module of NSG must align the graph representation G of the task (generated by the semantic parser) with the video. To that end, it first segments the video, then jointly learns a) the query encoders, which detect the queries in the video segments and b) the alignment between video segments and the query sequences obtained from the topological sort on G . Such joint learning is required since the temporal locations of the queries in the video are unknown a priori requiring simultaneous detection and alignment. If the video is a positive match for the task encoded in G , at least one of the query sequences from G must temporally align perfectly with the video segments for successful task verification. Conversely, for negative matches, no query sequence from G would *completely* align with the video segments. Going forward, we use $\langle \rangle$ and (\cdot) to denote ordered pairs and sequences, respectively.

Video Segmentation: The video is segmented into non-overlapping segments³ with a moving window of arbitrary, but fixed size k^4

Joint Optimization: The objective of the optimization is to jointly learn the *alignment* Z between queries and video segments along with the *query encoders* f^θ . Given: a) the

³Since pretrained, off-the-shelf video segmentation models are limited to predefined action classes [13] or reliant on background frame change detection [73] and require downstream finetuning [15], we leave their integration in NSG as future work.

⁴If required, the last segment is zero-padded to k frames.

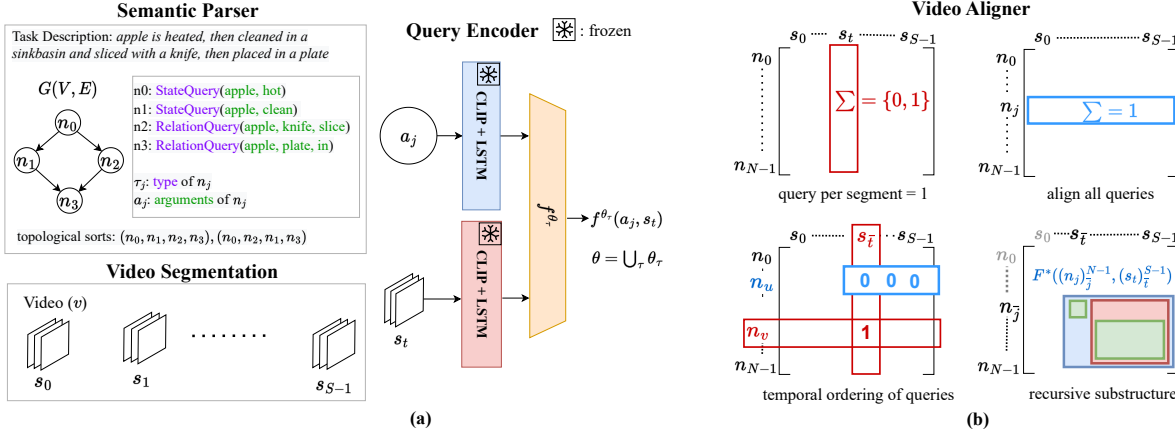


Figure 4. **NSG model** (a) semantic parser converts NL descriptions into a graph G of symbolic queries; query encoders f^{θ_τ} detect queries in individual video segments s_t ; and a video aligner aligns G with video segments by computing alignment matrix Z via a constrained optimization problem (Eq. 3). (b) The constraints (Eqs. 3a 3b 3c) and the recursive structure (Eq. 4) enabling use of DP to solve for Z . Here, the blue box denotes $F^*((n_j)_{\bar{j}}^{N-1}, (s_t)_{\bar{t}}^{S-1})$, the green boxes denote $\log f^\theta(a_{\bar{j}}, s_{\bar{t}}) + F^*((n_j)_{\bar{j}+1}^{N-1}, (s_t)_{\bar{t}+1}^{S-1})$, and the red box denotes $F^*((n_j)_{\bar{j}}^{N-1}, (s_t)_{\bar{t}+1}^{S-1})$.

temporal sequence of S segments $(s_t)_{t=0}^{S-1}$ with each s_t spanning k image frames; and b) a sequence of N queries $(n_j)_{j=0}^{N-1}$ from the topological sort on G , the alignment Z is defined as a matrix $Z \in \{0, 1\}^{N \times S}$, where $Z_{jt} = 1$ implies that the j^{th} query n_j is aligned the video segment s_t . An example alignment with $N = 2$ and $S = 3$ is given by the matrix $Z = \begin{bmatrix} 1 & 0 & 0 \\ 0 & 0 & 1 \end{bmatrix}$, where the rows are ordered queries (n_0, n_1) , the columns are temporal segments (s_0, s_1, s_2) , and $\langle n_0, s_0 \rangle, \langle n_1, s_2 \rangle$ are the aligned pairs. Assuming segmentation guarantees sufficient segments for query alignment: $S \geq N$. Using Z and f^θ , the task verification probability p^θ can be defined as:

$$p^\theta = \sigma \left(\max_{Z \in \{0, 1\}^{N \times S}} \frac{1}{N} \sum_{j, t} \log f^\theta(a_j, s_t) Z_{jt} \right) \quad (1)$$

Here σ is the sigmoid function, $f^\theta(a_j, s_t)$ denotes the probability of querying segment s_t using query n_j with arguments a_j (§ 5.3), and max operator is over the best alignment Z between N queries and S segments. We use the ground-truth task verification label y to compute Z and f^θ by minimizing the following loss:

$$\min_{\theta} \frac{1}{|\mathcal{D}|} \sum \mathcal{L}_{\text{BCE}}(p^\theta, y), \quad (2)$$

here $|\mathcal{D}|$ is the EgoTV dataset size and $\mathcal{L}_{\text{BCE}}(\cdot)$ is the binary cross entropy loss computed over $|\mathcal{D}|$ input, output pairs. Given the minimax nature of Eq. 2, we use a 2-step iterative optimization process: (i) find the best alignment Z between queries and segments with fixed query encoder parameters θ (optimize Eq. 1 with fixed f^θ); (ii) optimize θ using Eq. 2, given Z .

Dynamic Programming (DP)-based Alignment: Finding the best Z in Eq. 1 given θ requires iterating over combinations of N queries and S segments while respecting certain constraints. The constraints, visualized in Fig. 4b, ensure that a) no two queries are aligned to the same segment⁵ (Eq. 3a), b) all queries are accounted for in S (Eq. 3b), and c) the temporal orderings between queries in the query sequences are respected (Eq. 3c). Specifically, if query n_u precedes n_v ($n_u \rightarrow n_v$), and query n_v is paired with segment $s_{\bar{t}}$ (i.e. $Z_{v\bar{t}} = 1$), then query n_u cannot be paired with any segment that lies after $s_{\bar{t}}$ (i.e. $Z_{ut} \neq 1 \forall t \geq \bar{t}$). The resulting optimization problem for Z , given θ is:

$$\max_{Z \in \{0, 1\}^{N \times S}} \sum_{j, t} \log f^\theta(a_j, s_t) Z_{jt}, \quad \text{s.t.} \quad (3)$$

$$\sum_{j=0}^{N-1} Z_{jt} \in \{0, 1\}, \quad \forall 0 \leq t \leq S-1 \quad (3a)$$

$$\sum_{t=0}^{S-1} Z_{jt} = 1, \quad \forall 0 \leq j \leq N-1 \quad (3b)$$

$$n_u \rightarrow n_v, \quad Z_{v\bar{t}} = 1 \implies Z_{ut} \neq 1, \quad \forall t \geq \bar{t} \quad (3c)$$

Intuitively, the solution to Eq. 3 gives us the best alignment score (note, the overlap with Eq. 1). The iterations over N queries and S segments for solving Eq. 3 are underpinned by an overlapping and optimal substructure. For instance, to optimally align queries $(n_j)_{j=0}^{N-1}$ and segments $(s_t)_{t=0}^{S-1}$, one could: a) pair $\langle n_0, s_0 \rangle$ and optimally align the remaining queries and segments $(n_j)_{j=1}^{N-1}, (s_t)_{t=1}^{S-1}$, or (2)

⁵This ensures that the order of queries can be verified, which cannot be done when queries belong to the same segment.

skip s_0 and still optimally align *all* queries, now with the remaining segments $(n_j)_{j=0}^{N-1}, (s_t)_{t=1}^{S-1}$ (see Fig. 4b(iv)). This recursive substructure leads to a DP solution for Eq. 3.

Let, $F^*((n_j)_{\bar{j}}^{N-1}, (s_t)_{\bar{t}}^{S-1})$ denote the best alignment score for queries $(n_j)_{\bar{j}}^{N-1}$ and segments $(s_t)_{\bar{t}}^{S-1}$ from Eq. 3. Based on the aforementioned reasoning, $F^*((n_j)_{\bar{j}}^{N-1}, (s_t)_{\bar{t}}^{S-1})$ can be recursively written as:

$$\begin{aligned} F^*((n_j)_{\bar{j}}^{N-1}, (s_t)_{\bar{t}}^{S-1}) &= \max(\log f^\theta(a_{\bar{j}}, s_{\bar{t}}) \\ &+ F^*((n_j)_{\bar{j}+1}^{N-1}, (s_t)_{\bar{t}+1}^{S-1}), F^*((n_j)_{\bar{j}}^{N-1}, (s_t)_{\bar{t}+1}^{S-1})) \end{aligned} \quad (4)$$

The base cases for the DP are: (i) $Z = \mathbb{I}$ if $N = S$; (ii) $Z_{jt} = 1 \forall t$ if $j = N - 1$. It is worth noting that the DP subproblems, together with the base cases, satisfy the constraints in Eq. 3a 3b 3c. Since the video may match any of the sequence in the super-set of query sequences (from the topological sort on G), we repeat this process of computing F^* for each sequence and select the maximum value.

Optimizing Query Encoder Parameters θ : After obtaining the best alignment Z using DP, we substitute the corresponding value of $F^*((n_j)_{j=0}^{N-1}, (s_t)_{t=0}^{S-1})$ in Eq. 1 and subsequently Eq. 2. In Eq. 2, we use single mini-batch of training examples and take one gradient-update step of the Adam optimizer for the query encoder parameters θ .

6. Experiments

We compare various state-of-the-art (SOTA) VLMs with NSG on the EgoTV benchmark (see Appendix 10.1 for NSG’s experimental training details).

6.1. SOTA VLM Baselines

We investigate 6 VLMs developed for video-language tasks requiring similar reasoning as EgoTV. Summarized in Table 3, **CLIP4Clip** [39], **CLIP Hitchhiker** [3], **CoCa** [76] use image backbones followed by temporal aggregation, while **VideoCLIP** [36], **MIL-NCE** [44], and **VIOLIN** [38] use video backbones. With the exception of CoCa, which is trained with contrastive and captioning loss, all other models are trained using contrastive loss [44]. Lastly, VideoCLIP and VIOLIN use an explicit fusion of text-vision features. For each model, we freeze all pretrained feature extractors and finetune a fully-connected probe layer, along with the temporal aggregation layers where appropriate (CLIP4Clip-LSTM, VIOLIN), using EgoTV’s train split.

Finally, to establish upper bounds on EgoTV, we instantiate: (1) a **Text2text model**, which constructs video captions using ground-truth labels for objects and actions, encodes the captions and task descriptions using (pretrained) RoBERTa model [81] and measures alignment using the cosine similarity score (see Appendix 11.2), and (2) an **Oracle model**, which is trained with full supervision on sub-tasks labels and locations in addition to task verification labels.

6.2. Results

In Table 3, we show the performance of NSG vs. SOTA VLMs per split of EgoTV. (1) **Novel Tasks:** NSG significantly outperforms other baselines due to its ability to decompose and detect sub-tasks while using DP alignment to handle temporal constraints among them. In contrast, other baselines rely on detecting the entire task under temporal constraints, which is more challenging. Further, image-based baselines outperform video-based baselines due to their ability to capture a greater degree of compositional detail through frame-level representations. (2) **Novel Steps:** NSG’s poor performance in this split could be attributed to its low precision in the *slice* sub-task (which is dominant in this split), as shown in Figure 5 [Right]. We hypothesize that since NSG only uses the aligned segments while discarding the rest, learning to utilize context from neighboring segments to capture *slice* (like picking up a knife) could be a promising future direction. (3) **Novel Scenes:** Here, NSG is comparable to the best baseline VIOLIN-ResNet. Since the tasks are identical to the train split, the success of a model is contingent on the vision encoder’s ability to accurately detect the same sub-tasks in unseen scenes. Consequently, models with an additional temporal aggregation layer (VIOLIN) finetuned on EgoTV, tend to outperform image-based models that do not have temporal aggregation (CLIP Hitchhiker) and models with frozen video features (MIL-NCE, VideoCLIP). (4) **Abstraction:** NSG significantly outperforms the baselines, primarily due to its semantic parser, which captures the underlying structure of the description and encodes the relevant concepts, such as objects and sub-tasks, to generate an (abstract) symbolic output.

6.3. Analysis of NSG

NSG learns to localize task-relevant entities without explicit supervision. Figure 5 shows the confusion matrix of `StateQuery` & `RelationQuery` outputs, which capture sub-tasks, with their ground truths. The high recall demonstrates NSG’s ability to localize task-relevant entities, despite being trained using only task verification labels.

Effect of query types on NSG. While query types with multiple entity arguments might appear capable of modeling complex dependencies amongst entities and having more expressive power, encoding multiple entities jointly using a single encoder makes the grounding problem more challenging. Hence, in practice, we found that using a combination of `StateQuery` & `RelationQuery` types as opposed to `ActionQuery` (which encodes multiple entities using a single encoder) enabled better grounding and led to better performance in terms of F1-score (Table 4).

NSG shows consistent performance with increasing task difficulty. In Figure 5, NSG’s performance is minimally affected by increase in task difficulty characterized by number of sub-tasks (complexity) and ordering constraints (§ 3.2.2)

Model	Visual feature	Text feature	MM Fusion	Novel Tasks	Novel Steps	Novel Scenes	Abstraction	Average
Text2text [81]		RoBERTa		64.9	65.8	66.5	64.7	65.5
CLIP Hitchhiker [3]	CLIP(I)	CLIP		43.9	66.5	72.2	13.6	49.1
CLIP4Clip mean [39]	CLIP(I)	CLIP		49.3	70.9	74.9	16.1	52.8
CLIP4Clip seqLSTM [39]	CLIP(I)	CLIP		<u>56.2</u>	73.2	74.6	17.5	55.4
CoCa [76]	Tx(I)	Tx	Y	51.5	71.6	71.9	43.5	59.6
VIOLIN-ResNet [38]	ResNet(I)	BERT	Y	47.4	80.4	85.6	42.5	64.0
MIL-NCE [44]	S3D(V)	Word2vec		30.5	69.6	73.5	24.3	49.5
VideoCLIP [36]	Tx(V)	Tx	Y	29.3	67.6	77.9	25.6	50.1
VIOLIN-I3D [38]	I3D(V)	BERT	Y	45.6	<u>79.7</u>	83.9	<u>47.6</u>	64.2
NSG (ours)	CLIP(I)	CLIP	Y	90.0	64.7	84.9	80.4	80.0
Oracle Model	CLIP(I)	CLIP	Y	95.0	96.7	97.6	97.2	96.6

Table 3. **Comparison of baselines with NSG on different data splits using F1-score.** MM fusion indicates multimodal fusion of vision and text features. Tx indicates the Transformer as feature extractor with image (I) and video (V) backbones. Video backbone models are highlighted in gray. Underline indicates second-best performance.

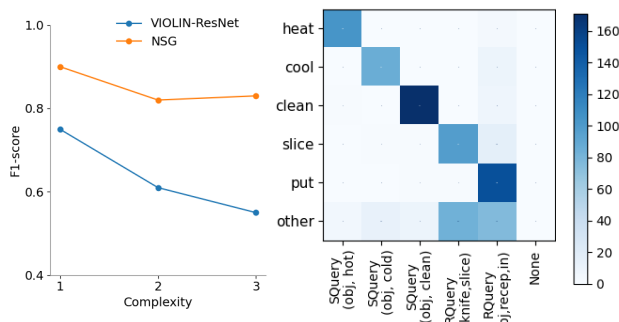


Figure 5. [Left] F1-score of NSG vs. best-performing baseline for EgoTV tasks with varying complexity averaged over all splits (Appendix 10.4 shows performance with varying ordering). [Right] Confusion Matrix for NSG Queries on validation split (SQuery: StateQuery, RQuery: RelationQuery). See Appendix 10.4 for results on all splits.

NSG	Novel Tasks	Novel Steps	Novel Scenes	Abstract.
Action	78.2	45.6	70.6	75.5
State+Relation	90.0	64.7	84.9	80.4

Table 4. (State + Relation) Query vs. ActionQuery

unlike the best-performing baseline (VIOLIN-ResNet).

NSG is robust to segmentation window size The effect of k on NSG is minimal (Appendix 10.4).

NSG also enables task verification on real-world data.

NSG outperforms all competitive baselines on CTV significantly with F1-score (NSG: **76.3**, CoCa: 70.9, VideoCLIP: 49.7, VIOLIN 34.7), demonstrating its causal and compositional reasoning capabilities in real-world applications (see Appendix 10.4 for details).

Limitations of NSG. (1) It does not consider multiple simultaneous actions like “picking an apple while closing the refrigerator door”, (2) The assumption of equal-length

video segments may be unsuitable for sub-tasks with a highly variable duration. We defer exploration of these limitations to future work, (3) Since NSG aligns the video with the entire task graph, it requires the full task execution video. Without this, alignment is partial, rendering NSG ineffective for online task verification.

7. Conclusion

To address various challenges towards the development of egocentric assistants that can track and verify the accomplishment of everyday tasks, including reasoning about causal and temporal constraints in tasks, visual grounding, and compositional generalization, we introduce Egocentric Task Verification (EgoTV), a benchmark and dataset containing partially-ordered, multi-step tasks with natural language task specifications. We also present NSG, a novel neuro-symbolic approach that enables order-aware visual grounding, and demonstrate its effectiveness on both the EgoTV dataset and a real-world dataset CTV. We hope our contributions will help in advancing research on egocentric assistants that can aid users in everyday tasks.

Acknowledgement

This work was partially supported by the Wallenberg AI, Autonomous Systems and Software Program (WASP) funded by the Knut and Alice Wallenberg Foundation.

References

- [1] Zeina Abu-Aisheh, Romain Raveaux, Jean-Yves Ramel, and Patrick Martineau. An exact graph edit distance algorithm for solving pattern recognition problems. In *Proceedings of the International Conference on Pattern Recognition Applications and Methods - Volume 1*, ICPRAM 2015, page 271–278, Setubal, PRT, 2015. SCITEPRESS - Science and Technology Publications, Lda.

[2] Saeed Amizadeh, Hamid Palangi, Alex Polozov, Yichen Huang, and Kazuhito Koishida. Neuro-symbolic visual reasoning: Disentangling. In *International Conference on Machine Learning*, pages 279–290. PMLR, 2020.

[3] Max Bain, Arsha Nagrani, GÜl Varol, and Andrew Zisserman. A clip-hitchhiker’s guide to long video retrieval. *arXiv preprint arXiv:2205.08508*, 2022.

[4] Siddhant Bansal, Chetan Arora, and CV Jawahar. My view is the best view: Procedure learning from egocentric videos. In *Computer Vision–ECCV 2022: 17th European Conference, Tel Aviv, Israel, October 23–27, 2022, Proceedings, Part XIII*, pages 657–675. Springer, 2022.

[5] Fabien Baradel, Natalia Neverova, Julien Mille, Greg Mori, and Christian Wolf. Cophy: Counterfactual learning of physical dynamics. In *International Conference on Learning Representations*, 2020.

[6] Ben Beglin, Sanjay Subramanian, Matt Gardner, and Jonathan Berant. Latent Compositional Representations Improve Systematic Generalization in Grounded Question Answering. *Transactions of the Association for Computational Linguistics*, 9:195–210, 03 2021.

[7] João Carreira and Andrew Zisserman. Quo vadis, action recognition? a new model and the kinetics dataset. In *2017 IEEE Conference on Computer Vision and Pattern Recognition (CVPR)*, pages 4724–4733, 2017.

[8] Zhenfang Chen, Jiayuan Mao, Jiajun Wu, Kwan-Yee Kenneth Wong, Joshua B. Tenenbaum, and Chuang Gan. Grounding physical concepts of objects and events through dynamic visual reasoning. In *International Conference on Learning Representations*, 2021.

[9] Ido Dagan, Oren Glickman, and Bernardo Magnini. The pascal recognising textual entailment challenge. In *Machine Learning Challenges. Evaluating Predictive Uncertainty, Visual Object Classification, and Recognising Tectual Entailment: First PASCAL Machine Learning Challenges Workshop, MLCW 2005, Southampton, UK, April 11-13, 2005, Revised Selected Papers*, pages 177–190. Springer, 2006.

[10] Dima Damen, Hazel Doughty, Giovanni Maria Farinella, Sanja Fidler, Antonino Furnari, Evangelos Kazakos, Davide Moltisanti, Jonathan Munro, Toby Perrett, Will Price, and Michael Wray. The epic-kitchens dataset: Collection, challenges and baselines. *IEEE Transactions on Pattern Analysis and Machine Intelligence (TPAMI)*, 43(11):4125–4141, 2021.

[11] Samyak Datta, et al. Episodic memory question answering. In *CVPR*, pages 19119–19128, 2022.

[12] Jacob Devlin, Ming-Wei Chang, Kenton Lee, and Kristina Toutanova. BERT: Pre-training of deep bidirectional transformers for language understanding. In *Proceedings of the 2019 Conference of the North American Chapter of the Association for Computational Linguistics: Human Language Technologies, Volume 1 (Long and Short Papers)*, pages 4171–4186, Minneapolis, Minnesota, June 2019. Association for Computational Linguistics.

[13] Victor Escorcia, Fabian Caba Heilbron, Juan Carlos Niebles, and Bernard Ghanem. Daps: Deep action proposals for action understanding. In *European conference on computer vision*, pages 768–784. Springer, 2016.

[14] Alireza Fathi and James M Rehg. Modeling actions through state changes. In *Proceedings of the IEEE Conference on Computer Vision and Pattern Recognition*, pages 2579–2586, 2013.

[15] Jialin Gao, Zhixiang Shi, Guanshuo Wang, Jian Li, Yufeng Yuan, Shiming Ge, and Xi Zhou. Accurate temporal action proposal generation with relation-aware pyramid network. In *Proceedings of the AAAI conference on artificial intelligence*, volume 34, pages 10810–10817, 2020.

[16] Rohit Girdhar and Deva Ramanan. CATER: A diagnostic dataset for Compositional Actions and TEmporal Reasoning. In *ICLR*, 2020.

[17] Kristen Grauman, Andrew Westbury, Eugene Byrne, Zachary Chavis, Antonino Furnari, Rohit Girdhar, Jackson Hamburger, Hao Jiang, Miao Liu, Xingyu Liu, Miguel Martin, Tushar Nagarajan, Ilija Radosavovic, Santhosh Kumar Ramakrishnan, Fiona Ryan, Jayant Sharma, Michael Wray, Mengmeng Xu, Eric Zhongcong Xu, Chen Zhao, Siddhant Bansal, Dhruv Batra, Vincent Cartillier, Sean Crane, Tien Do, Morrie Doulaty, Akshay Erapalli, Christoph Feichtenhofer, Adriano Fragnani, Qichen Fu, Abrham Gebreslasie, Cristina González, James Hillis, Xuhua Huang, Yifei Huang, Wenqi Jia, Leslie Khoo, Jáchym Kolář, Satwik Kottur, Anurag Kumar, Federico Landini, Chao Li, Yanghao Li, Zhenqiang Li, Karttikeya Mangalam, Raghava Modhug, Jonathan Munro, Tullie Murrell, Takumi Nishiyasu, Will Price, Paola Ruiz Puentes, Merey Ramazanova, Leda Sari, Kiran Somasundaram, Audrey Southerland, Yusuke Sugano, Ruijie Tao, Minh Vo, Yuchen Wang, Xindi Wu, Takuma Yagi, Ziwei Zhao, Yunyi Zhu, Pablo Arbeláez, David Crandall, Dima Damen, Giovanni Maria Farinella, Christian Fuegen, Bernard Ghanem, Vamsi Krishna Ithapu, C. V. Jawahar, Hanbyul Joo, Kris Kitani, Haizhou Li, Richard Newcombe, Aude Oliva, Hyun Soo Park, James M. Rehg, Yoichi Sato, Jianbo Shi, Mike Zheng Shou, Antonio Torralba, Lorenzo Torresani, Mingfei Yan, and Jitendra Malik. Ego4d: Around the world in 3,000 hours of egocentric video. In *2022 IEEE/CVF Conference on Computer Vision and Pattern Recognition (CVPR)*, pages 18973–18990, 2022.

[18] Madeleine Grunde-McLaughlin, Ranjay Krishna, and Maneesh Agrawala. Agqa: A benchmark for compositional spatio-temporal reasoning. In *2021 IEEE/CVF Conference on Computer Vision and Pattern Recognition (CVPR)*, pages 11282–11292, 2021.

[19] Kaiming He, Xiangyu Zhang, Shaoqing Ren, and Jian Sun. Deep residual learning for image recognition. In *2016 IEEE Conference on Computer Vision and Pattern Recognition (CVPR)*, pages 770–778, 2016.

[20] FC Heilbron, V Escorcia, B Ghanem, and J Niebles. A large-scale video benchmark for human activity understanding. In *Proceedings of the IEEE Conference on Computer Vision and Pattern Recognition, Boston, 2015*, 961, volume 970, 2019.

[21] Fabian Caba Heilbron, Victor Escorcia, Bernard Ghanem, and Juan Carlos Niebles. Activitynet: A large-scale video benchmark for human activity understanding. In *2015 IEEE Conference on Computer Vision and Pattern Recognition (CVPR)*, pages 961–970, 2015.

[22] Sepp Hochreiter and Jürgen Schmidhuber. Long short-term memory. *Neural computation*, 9(8):1735–1780, 1997.

[23] Jörg Hoffmann. The Metric-FF planning system: Translating “ignoring delete lists” to numeric state variables. *Journal of Artificial Intelligence Research*, 20:291–341, 2003.

[24] De-An Huang, Suraj Nair, Danfei Xu, Yuke Zhu, Animesh Garg, Li Fei-Fei, Silvio Savarese, and Juan Carlos Niebles. Neural task graphs: Generalizing to unseen tasks from a single video demonstration. In *Proceedings of the IEEE/CVF conference on computer vision and pattern recognition*, pages 8565–8574, 2019.

[25] Jingwei Ji, Ranjay Krishna, Li Fei-Fei, and Juan Carlos Niebles. Action genome: Actions as compositions of spatio-temporal scene graphs. In *Proceedings of the IEEE/CVF Conference on Computer Vision and Pattern Recognition*, pages 10236–10247, 2020.

[26] Baoxiong Jia, Ting Lei, Song-Chun Zhu, and Siyuan Huang. Egotaskqa: Understanding human tasks in egocentric videos. In *The 36th Conference on Neural Information Processing Systems (NeurIPS 2022) Track on Datasets and Benchmarks*, 2022.

[27] Yu-Gang Jiang, Jingen Liu, A Roshan Zamir, George Toderici, Ivan Laptev, Mubarak Shah, and Rahul Sukthankar. Thumos challenge: Action recognition with a large number of classes. <http://crcv.ucf.edu/THUMOS14/>, 2014.

[28] Diederik P Kingma and Jimmy Ba. Adam: A method for stochastic optimization. *arXiv preprint arXiv:1412.6980*, 2014.

[29] Eric Kolve, Roozbeh Mottaghi, Winson Han, Eli VanderBilt, Luca Weihs, Alvaro Herrasti, Daniel Gordon, Yuke Zhu, Abhinav Gupta, and Ali Farhadi. AI2-THOR: An Interactive 3D Environment for Visual AI. *arXiv*, 2017.

[30] Juho Lee, Yoonho Lee, Jungtaek Kim, Adam Kosiorek, Seungjin Choi, and Yee Whye Teh. Set transformer: A framework for attention-based permutation-invariant neural networks. In *International conference on machine learning*, pages 3744–3753. PMLR, 2019.

[31] Jie Lei, Licheng Yu, Mohit Bansal, and Tamara Berg. TVQA: Localized, compositional video question answering. In *Proceedings of the 2018 Conference on Empirical Methods in Natural Language Processing*, pages 1369–1379, Brussels, Belgium, Oct.-Nov. 2018. Association for Computational Linguistics.

[32] Junnan Li, Dongxu Li, Caiming Xiong, and Steven Hoi. Blip: Bootstrapping language-image pre-training for unified vision-language understanding and generation. In *International Conference on Machine Learning*, pages 12888–12900. PMLR, 2022.

[33] Jiangtong Li, Li Niu, and Liqing Zhang. From representation to reasoning: Towards both evidence and commonsense reasoning for video question-answering. In *Proceedings of the IEEE/CVF Conference on Computer Vision and Pattern Recognition (CVPR)*, June 2022.

[34] Linjie Li, Yen-Chun Chen, Yu Cheng, Zhe Gan, Licheng Yu, and Jingjing Liu. Hero: Hierarchical encoder for video+language omni-representation pre-training. *arXiv preprint arXiv:2005.00200*, 2020.

[35] Liunian Harold Li, Pengchuan Zhang, Haotian Zhang, Jianwei Yang, Chunyuan Li, Yiwu Zhong, Lijuan Wang, Lu Yuan, Lei Zhang, Jenq-Neng Hwang, et al. Grounded language-image pre-training. In *Proceedings of the IEEE/CVF Conference on Computer Vision and Pattern Recognition*, pages 10965–10975, 2022.

[36] Yikang Li, Jenhao Hsiao, and Chiuaman Ho. Videoclip: A cross-attention model for fast video-text retrieval task with image clip. In *Proceedings of the 2022 International Conference on Multimedia Retrieval*, pages 29–33, 2022.

[37] Xudong Lin, Fabio Petroni, Gedas Bertasius, Marcus Rohrbach, Shih-Fu Chang, and Lorenzo Torresani. Learning to recognize procedural activities with distant supervision. In *Proceedings of the IEEE/CVF Conference on Computer Vision and Pattern Recognition*, pages 13853–13863, 2022.

[38] J. Liu, Wenhui Chen, Yu Cheng, Zhe Gan, Licheng Yu, Yiming Yang, and Jingjing Liu. Violin: A large-scale dataset for video-and-language inference. *2020 IEEE/CVF Conference on Computer Vision and Pattern Recognition (CVPR)*, pages 10897–10907, 2020.

[39] Huaishao Luo, Lei Ji, Ming Zhong, Yang Chen, Wen Lei, Nan Duan, and Tianrui Li. Clip4clip: An empirical study of clip for end to end video clip retrieval and captioning. *Neurocomputing*, 508:293–304, 2022.

[40] Four optics breakthroughs to power enterprise ar - magic leap. <https://www.magicleap.com/en-us/>.

[41] Jiayuan Mao, Chuang Gan, Pushmeet Kohli, Joshua B. Tenenbaum, and Jiajun Wu. The Neuro-Symbolic Concept Learner: Interpreting Scenes, Words, and Sentences From Natural Supervision. In *International Conference on Learning Representations*, 2019.

[42] Weichao Mao, Ruta Desai, Michael Louis Iuzzolino, and Nitin Kamra. Action dynamics task graphs for learning plannable representations of procedural tasks. *arXiv preprint arXiv:2302.05330*, 2023.

[43] Mexionaction2: action detection and localization dataset. <http://mexculture.cnam.fr/xwiki/bin/view/Datasets/Mex+action+dataset>.

[44] Antoine Miech, Jean-Baptiste Alayrac, Lucas Smaira, Ivan Laptev, Josef Sivic, and Andrew Zisserman. End-to-end learning of visual representations from uncurated instructional videos. In *Proceedings of the IEEE/CVF Conference on Computer Vision and Pattern Recognition*, pages 9879–9889, 2020.

[45] Tomas Mikolov, Kai Chen, Greg Corrado, and Jeffrey Dean. Efficient estimation of word representations in vector space. In *arXiv preprint arXiv:1301.3781*, 2013.

[46] OpenAI.

[47] Aishwarya Padmakumar, Jesse Thomason, Ayush Shrivastava, Patrick Lange, Anjali Narayan-Chen, Spandana Gella, Robinson Piramuthu, Gokhan Tur, and Dilek Hakkani-Tur. Teach: Task-driven embodied agents that chat. In *Proceedings of the AAAI Conference on Artificial Intelligence*, volume 36, pages 2017–2025, 2022.

[48] Jeffrey Pennington, Richard Socher, and Christopher Manning. GloVe: Global vectors for word representation. In *Proceedings of the 2014 Conference on Empirical Methods in*

Natural Language Processing (EMNLP), pages 1532–1543, Doha, Qatar, Oct. 2014. Association for Computational Linguistics.

[49] Yicheng Qian, Weixin Luo, Dongze Lian, Xu Tang, Peilin Zhao, and Shenghua Gao. Svip: Sequence verification for procedures in videos. In *Proceedings of the IEEE/CVF Conference on Computer Vision and Pattern Recognition*, pages 19890–19902, 2022.

[50] Alec Radford, Jong Wook Kim, Chris Hallacy, Aditya Ramesh, Gabriel Goh, Sandhini Agarwal, Girish Sastry, Amanda Askell, Pamela Mishkin, Jack Clark, Gretchen Krueger, and Ilya Sutskever. Learning transferable visual models from natural language supervision. In Marina Meila and Tong Zhang, editors, *Proceedings of the 38th International Conference on Machine Learning*, volume 139 of *Proceedings of Machine Learning Research*, pages 8748–8763. PMLR, 18–24 Jul 2021.

[51] Colin Raffel, Noam Shazeer, Adam Roberts, Katherine Lee, Sharan Narang, Michael Matena, Yanqi Zhou, Wei Li, and Peter J. Liu. Exploring the limits of transfer learning with a unified text-to-text transformer. *Journal of Machine Learning Research*, 21(140):1–67, 2020.

[52] Michaela Regneri, Marcus Rohrbach, Dominikus Wetzel, Stefan Thater, Bernt Schiele, and Manfred Pinkal. Grounding action descriptions in videos. *Transactions of the Association for Computational Linguistics*, 1:25–36, 2013.

[53] Keisuke Sakaguchi, Chandra Bhagavatula, Ronan Le Bras, Niket Tandon, Peter Clark, and Yejin Choi. proScript: Partially ordered scripts generation. In *Findings of the Association for Computational Linguistics: EMNLP 2021*, pages 2138–2149, Punta Cana, Dominican Republic, Nov. 2021. Association for Computational Linguistics.

[54] Md. Kamruzzaman Sarker, Lu Zhou, Aaron Eberhart, and Pascal Hitzler. Neuro-symbolic artificial intelligence: Current trends. *CoRR*, abs/2105.05330, 2021.

[55] Min Joon Seo, Aniruddha Kembhavi, Ali Farhadi, and Hannaneh Hajishirzi. Bidirectional attention flow for machine comprehension. In *5th International Conference on Learning Representations, ICLR 2017, Toulon, France, April 24–26, 2017, Conference Track Proceedings*. OpenReview.net, 2017.

[56] Yuhang Shen, Lu Wang, and Ehsan Elhamifar. Learning to segment actions from visual and language instructions via differentiable weak sequence alignment. In *Proceedings of the IEEE/CVF Conference on Computer Vision and Pattern Recognition*, pages 10156–10165, 2021.

[57] Mohit Shridhar, Jesse Thomason, Daniel Gordon, Yonatan Bisk, Winson Han, Roozbeh Mottaghi, Luke Zettlemoyer, and Dieter Fox. ALFRED: A Benchmark for Interpreting Grounded Instructions for Everyday Tasks. In *The IEEE Conference on Computer Vision and Pattern Recognition (CVPR)*, 2020.

[58] Gunnar A. Sigurdsson, Gü̈l Varol, Xiaolong Wang, Ali Farhadi, Ivan Laptev, and Abhinav Gupta. Hollywood in homes: Crowdsourcing data collection for activity understanding. In Bastian Leibe, Jiri Matas, Nicu Sebe, and Max Welling, editors, *Computer Vision – ECCV 2016*, pages 510–526, Cham, 2016. Springer International Publishing.

[59] Mattia Soldan, Alejandro Pardo, Juan León Alcázar, Fabian Caba Heilbron, Chen Zhao, Silvio Giancola, and Bernard Ghanem. Mad: A scalable dataset for language grounding in videos from movie audio descriptions. *arXiv preprint arXiv:2112.00431*, 2021.

[60] Tomáš Souček, Jean-Baptiste Alayrac, Antoine Miech, Ivan Laptev, and Josef Sivic. Look for the change: Learning object states and state-modifying actions from untrimmed web videos. In *Proceedings of the IEEE Conference on Computer Vision and Pattern Recognition (CVPR)*, June 2022.

[61] Sanjana Srivastava, Chengshu Li, Michael Lingelbach, Roberto Martín-Martín, Fei Xia, Kent Elliott Vainio, Zheng Lian, Cem Gokmen, Shyamal Buch, Karen Liu, Silvio Savarese, Hyowon Gweon, Jiajun Wu, and Li Fei-Fei. Behavior: Benchmark for everyday household activities in virtual, interactive, and ecological environments. In Aleksandra Faust, David Hsu, and Gerhard Neumann, editors, *Proceedings of the 5th Conference on Robot Learning*, volume 164 of *Proceedings of Machine Learning Research*, pages 477–490. PMLR, 08–11 Nov 2022.

[62] Yansong Tang, Dajun Ding, Yongming Rao, Yu Zheng, Danyang Zhang, Lili Zhao, Jiwen Lu, and Jie Zhou. Coin: A large-scale dataset for comprehensive instructional video analysis. In *Proceedings of the IEEE/CVF Conference on Computer Vision and Pattern Recognition*, pages 1207–1216, 2019.

[63] Makarand Tapaswi, Yukun Zhu, Rainer Stiefelhagen, Antonio Torralba, Raquel Urtasun, and Sanja Fidler. Movieqa: Understanding stories in movies through question-answering. In *2016 IEEE Conference on Computer Vision and Pattern Recognition (CVPR)*, pages 4631–4640, 2016.

[64] Tristan Thrush, Ryan Jiang, Max Bartolo, Amanpreet Singh, Adina Williams, Douwe Kiela, and Candace Ross. Winoground: Probing vision and language models for visiolinguistic compositionality. In *Proceedings of the IEEE/CVF Conference on Computer Vision and Pattern Recognition*, pages 5238–5248, 2022.

[65] Dorin Ungureanu, Federica Bogo, Silvano Galliani, Pooja Sama, Xin Duan, Casey Meekhof, Jan Stühmer, Thomas J Cashman, Bugra Tekin, Johannes L Schönberger, et al. Hololens 2 research mode as a tool for computer vision research. *arXiv preprint arXiv:2008.11239*, 2020.

[66] Jason Wei, Xuezhi Wang, Dale Schuurmans, Maarten Bosma, brian ichter, Fei Xia, Ed H. Chi, Quoc V Le, and Denny Zhou. Chain of thought prompting elicits reasoning in large language models. In Alice H. Oh, Alekh Agarwal, Danielle Belgrave, and Kyunghyun Cho, editors, *Advances in Neural Information Processing Systems*, 2022.

[67] Laurence A Wolsey. *Integer programming*. John Wiley & Sons, 2020.

[68] Bo Wu, Shoubin Yu, Zhenfang Chen, Joshua B Tenenbaum, and Chuang Gan. Star: A benchmark for situated reasoning in real-world videos. In *Thirty-fifth Conference on Neural Information Processing Systems (NeurIPS)*, 2021.

[69] Junbin Xiao, Xindi Shang, Angela Yao, and Tat-Seng Chua. Next-qa: Next phase of question-answering to explaining temporal actions. In *Proceedings of the IEEE/CVF Conference on Computer Vision and Pattern Recognition (CVPR)*, 2022.

ence on Computer Vision and Pattern Recognition (CVPR), pages 9777–9786, June 2021.

[70] Ning Xie, Farley Lai, Derek Doran, and Asim Kadav. Visual entailment: A novel task for fine-grained image understanding. *arXiv preprint arXiv:1901.06706*, 2019.

[71] Saining Xie, Chen Sun, Jonathan Huang, Zhuowen Tu, and Kevin Murphy. Rethinking spatiotemporal feature learning: Speed-accuracy trade-offs in video classification. In Vittorio Ferrari, Martial Hebert, Cristian Sminchisescu, and Yair Weiss, editors, *Computer Vision – ECCV 2018*, pages 318–335, Cham, 2018. Springer International Publishing.

[72] Yaqi Xie, Chen Yu, Tongyao Zhu, Jinbin Bai, Ze Gong, and Harold Soh. Translating natural language to planning goals with large-language models. *arXiv preprint arXiv:2302.05128*, 2023.

[73] Haosen Yang, Wenhao Wu, Lining Wang, Sheng Jin, Boyang Xia, Hongxun Yao, and Huijie Huang. Temporal action proposal generation with background constraint. In *Proceedings of the AAAI conference on artificial intelligence*, volume 36, pages 3054–3062, 2022.

[74] Kexin Yi, Chuang Gan, Yunzhu Li, Pushmeet Kohli, Jiajun Wu, Antonio Torralba, and Joshua B. Tenenbaum. CLEVRER: collision events for video representation and reasoning. In *8th International Conference on Learning Representations, ICLR 2020, Addis Ababa, Ethiopia, April 26–30, 2020*. OpenReview.net, 2020.

[75] Kexin Yi, Jiajun Wu, Chuang Gan, Antonio Torralba, Pushmeet Kohli, and Joshua B. Tenenbaum. Neural-symbolic vqa: Disentangling reasoning from vision and language understanding. In *Proceedings of the 32nd International Conference on Neural Information Processing Systems, NIPS’18*, page 1039–1050, Red Hook, NY, USA, 2018. Curran Associates Inc.

[76] Jiahui Yu, Zirui Wang, Vijay Vasudevan, Legg Yeung, Mojtaba Seyedhosseini, and Yonghui Wu. Coca: Contrastive captioners are image-text foundation models. *Transactions on Machine Learning Research*, 2022.

[77] Mert Yuksekgonul, Federico Bianchi, Pratyusha Kalluri, Dan Jurafsky, and James Zou. When and why vision-language models behave like bags-of-words, and what to do about it? In *International Conference on Learning Representations*, 2023.

[78] Amir Zadeh, Michael Chan, Paul Pu Liang, Edmund Tong, and Louis-Philippe Morency. Social-iq: A question answering benchmark for artificial social intelligence. In *2019 IEEE/CVF Conference on Computer Vision and Pattern Recognition (CVPR)*, pages 8799–8809, 2019.

[79] Andy Zeng, Maria Attarian, brian ichter, Krzysztof Marcin Choromanski, Adrian Wong, Stefan Welker, Federico Tombari, Aveek Purohit, Michael S Ryoo, Vikas Sindhwani, Johnny Lee, Vincent Vanhoucke, and Pete Florence. Socratic models: Composing zero-shot multimodal reasoning with language. In *International Conference on Learning Representations*, 2023.

[80] Yiwu Zhong, Jianwei Yang, Pengchuan Zhang, Chunyuan Li, Noel Codella, Liunian Harold Li, Luwei Zhou, Xiyang Dai, Lu Yuan, Yin Li, et al. Regionclip: Region-based language-image pretraining. In *Proceedings of the IEEE/CVF Conference on Computer Vision and Pattern Recognition*, pages 16793–16803, 2022.

[81] Liu Zhuang, Lin Wayne, Shi Ya, and Zhao Jun. A robustly optimized BERT pre-training approach with post-training. In *Proceedings of the 20th Chinese National Conference on Computational Linguistics*, pages 1218–1227, Huhhot, China, Aug. 2021. Chinese Information Processing Society of China.

[82] Dimitri Zhukov, Jean-Baptiste Alayrac, Ramazan Gokberk Cinbis, David Fouhey, Ivan Laptev, and Josef Sivic. Cross-task weakly supervised learning from instructional videos. In *2019 IEEE/CVF Conference on Computer Vision and Pattern Recognition (CVPR)*, pages 3532–3540, 2019.

Appendix for “EgoTV 📺: Egocentric Task Verification from Natural Language Task Descriptions”

This appendix is organized as follows:

8. *EgoTV dataset*: Generation details, additional statistics.
9. *CrossTask Verification (CTV) dataset*: Details on generation process and evaluation.
10. *NSG*: Semantic parsing approaches, additional analysis and ablations, performance on CTV.
11. *Baselines*: Details on VLM and Oracle baselines.

8. EgoTV Dataset

8.1. Task-video Generation using PDDL Planner

To generate EgoTV tasks, we encode the final state of the objects achieved by an EgoTV task as the “goal state” for the Planning Domain Definition Language (PDDL) planner. Note that the ordering constraints of the tasks aren’t captured when the tasks are encoded as goal states for the PDDL planner in this manner. For instance, the tasks of *clean_then_heat(apple)* and *clean_and_heat(apple)* would have the same PDDL goal states. Consequently, we enforce ordering constraints for a given task using “pre-conditions” in PDDL. In the above example task of *clean_then_heat(apple)*, the *clean* sub-task would thus be the pre-condition for the *heat* sub-task. Apart from the tasks and object states, the agent state and environment dynamics – e.g., the *heat* sub-task changes the state of the target object to be hot – are also encoded in PDDL.

For each task, a random kitchen scene is picked and the agent is spawned in the corresponding AI2-THOR scene. The planner leverages the initial state and action definitions to generate a sequence of sub-tasks required to achieve the goal. Rather than simply selecting the best plan, which may not always reflect human-like behavior, we aim to mimic the less-than-optimal decision-making of humans by randomly selecting a plan from the top- k plans. This approach enables the inclusion of sub-tasks that may not be strictly necessary for achieving the goal. Furthermore, the partial-ordered nature of tasks enables different plan generations to achieve the same task, thus promoting diversity. We use the Fast Forward (FF) planner [23] to generate plans.

Apart from sequencing the sub-tasks appropriately for achieving a given task, the planner also ensures that the agent can navigate to the correct locations for each sub-task. For instance, to execute the *clean* sub-task, an agent typically requires using the sink in the kitchen and hence must navigate there. The generated plans thus consist of navigation and object interaction actions.

8.2. EgoTV Task-description Generation

The task descriptions corresponding to negative samples, where the task videos are not entailed by their descriptions, are created by either altering the sequence of sub-tasks in the positive template or by replacing some of them with alternative sub-tasks picked randomly from the remaining repertoire of sub-tasks (see Figure 1 where *heat* is replaced with *cool*). To ensure the practicality of an assistive agent that aids a human, we maintain the target object in the negative samples but vary the sub-tasks, as negative task descriptions on the sub-task level are more relevant than on the object level. For abstraction, we (i) omit the low-level details like *clean in the sinkbasin*, *cool in the fridge*; (ii) (some) task-oriented descriptions are changed to goal-oriented descriptions (*apple is heated and cleaned* \mapsto *hot, clean apple*).

An example template of task descriptions corresponding to the task *cool_then_clean* is [‘{obj} is cooled in a Fridge, then cleaned in a SinkBasin’, ‘{obj} is cleaned in a SinkBasin after cooling in a Fridge’, ‘{obj} is cooled in a Fridge before cleaning in a SinkBasin’]. While EgoTV already incorporates some diversity in task descriptions in this manner, we note that inclusion of more diverse free-form language descriptions in the dataset (possibly collected through crowdsourcing) would be a valuable future enhancement.

8.3. Dataset Analysis and Statistics

See Figure 6 for a comparison of video lengths and task description lengths across different splits. It can be observed that the Novel Tasks split has the longest videos (≈ 1.6 minutes) and task descriptions (≈ 12 words) owing to its compositional tasks. Additionally, the Abstraction split has the shortest task description (≈ 5 words), even for longer videos due to abstraction. We include all tasks of EgoTV in Table 8 at the end of the supplement. We also perform a detailed analysis of each split (Figure 11).

9. CrossTask Verification (CTV) Dataset

9.1. Dataset construction

We leverage the CrossTask dataset and its action step annotations to construct our CrossTask Verification dataset. Each video contains task descriptions that are obtained by concatenating the sequence of *action steps* annotations available in the original CrossTask dataset. For ease of

	Reasoning		Dataset Characteristics			Grounding	
	compositional	causal	language	egocentric	real-world	diagnostic tools	objects, relations
CLEVRER [74]	✓	✓	✓	✗	✗	✓	✓
Next-QA [69]	✗	✓	✓	✗	✓	✓	✓
AGQA [18]	✓	✗	✓	✗	✓	✓	✓
Activity	✗	✗	✓	✗	✓	✗	✓
Net-QA [21]	✗	✗	✓	✗	✓	✗	✓
STAR [68]	✓	✓	✓	✗	✓	✓	✓
CoPhy [5]	✗	✓	✗	✗	✗	✓	✓
Social-IQ [78]	✗	✓	✓	✗	✓	✓	✗
Causal-	✗	✓	✓	✗	✓	✓	✓
VidQA [33]	✗	✗	✓	✗	✓	✓	✓
Charades [58]	✗	✗	✓	✗	✓	✓	✓
CATER [16]	✓	✗	✗	✗	✗	✓	✓
EPIC-	✓	✓	✓	✓	✓	✓	✓
KITCHENS [10]	✓	✓	✓	✓	✓	✓	✓
Ego-4D [17]	✗	✓	✓	✓	✓	✓	✓
VIOLIN [38]	✗	✓	✓	✗	✓	✗	✓
Change-It [60]	✗	✓	✗	✓	✓	✗	✓
Cross-Task [82]	✓	✓	✓	✗	✓	✗	✓
EgoTV 	✓	✓	✓	✓	✗	✓	✓

Table 5. **EgoTV vs. existing video-language datasets.** EgoTV benchmark enables reasoning (compositional, causal, and temporal); has unique dataset characteristics along with diagnostics; requires grounding of objects, relations, and actions.

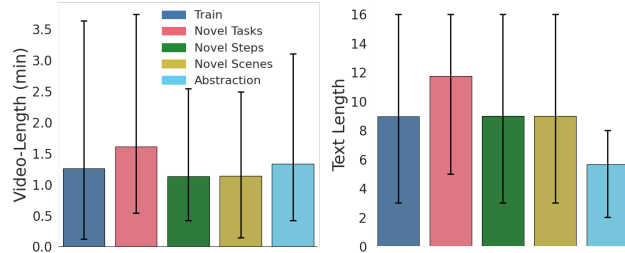


Figure 6. **Additional EgoTV dataset statistics.** Comparison of video length (in minutes) and task description length (number of words) across different splits using error plots. Novel Tasks split has the longest videos and task descriptions. Abstraction split has the shortest task descriptions.

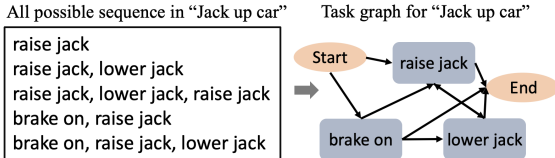


Figure 7. **Task graphs are used to create impossible sequences for generating negative task descriptions in the CTV dataset.**

experimentation, we only consider the top-4 frequent action steps for each task in CrossTask. Consequently, CTV dataset videos are constructed by selecting the segments corresponding to these frequent actions per video and are thus shorter than the original CrossTask videos.

We follow a process similar to EgoTV for generating **negative descriptions**: (i) *replacing action steps from other tasks*: where we substitute an action step in the sequence

with an action step in another task. (ii) *replacing action steps from the same task*: instead of replacing steps from another task, we reuse the unused action steps, which were not the top-4 frequent steps in the same task. These action steps are closer in semantics and serve as hard negative. (iii) *replacing action step sequence order to an impossible order*: we first list out all possible action step orders in CrossTask following [42] as shown in Figure 7. Then, we construct an action step sequence that doesn’t exist in CrossTask for the given task, e.g., *lower jack, upper jack, break on* for the task of *fixing the car*. We assume that these sequence orders are impossible since they were not observed in any videos for a given task.

Apart from generating negative NL task descriptions, we also generate **negative videos** in two ways: (i) *shuffling the video order corresponding to action step sequence*: this mimics the case where the action steps were not executed in the correct order. (ii) *dropping a video segment corresponding to an action step*: this corresponds to the situations where an action step is missed while executing the task, potentially resulting in a failure in accomplishing the task. Thus, this is an important use case for task verification.

10. NSG details

10.1. NSG Training details

When training NSG, we do not update the weights of the CLIP feature extractors (Sec. 5.3) due to GPU memory limitations. We use a batch of $N = 64$ samples, where we sample the video at 2.5 FPS. We set a window size $k = 20$ frames for segmentation in NSG (Sec. 5.4), each window

representing an 8-second video segment. We use a train-validation split of 80-20 and use the validation performance as an indicator of convergence. We minimize the binary cross-entropy loss in Eq. 2 with Adam [28] and a learning rate of 1e-3. Each model is trained on 8 V100 GPUs for 50 epochs for two days.

10.2. NSG Semantic Parsing

We test two semantic parsing methods: (i) Finetuning language models to generate graphs from NL descriptions; (ii) Few-shot prompting of large language models.

10.2.1 Finetuning Language Models

Recently, it has been shown that pre-trained language models can be leveraged for graph [53] and plan generation [72] from NL. We use a similar framework to train a T5-small transformer [51] to generate partial-ordered plans. For this, we use a subset of the training data (in particular the positive task descriptions for which we have gold-label graphs annotations) and annotate them with their partial-ordered plans in the form of directed acyclic graphs (DAG) – $G(V, E)$, where vertices $n_i \in V$ represent sub-tasks, and edges $e_{ij} \in E$ are ordering constraints that indicate n_i must precede n_j (i.e. $n_i \rightarrow n_j$). To train the text generation transformer, we represent the output graph in DOT language. The corresponding DOT representation for the graph in Figure 4 is given as:

```
Step 0: StateQuery(apple, hot),
Step 1: StateQuery(apple, clean),
Step 2: StateQuery(apple, sliced),
Step 3: RelationQuery(apple, plate, in),
Step 0 → Step 1, Step 0 → Step 2,
Step 1 → Step 3, Step 2 → Step 3
```

Ablations on Plan Generation framework: We assess the correctness of the graphs generated by the trained T5-transformer model on the positive task descriptions of our test splits. The evaluation metric is Graph Edit Distance (GED) [1] which computes the distance between two graphs (G_1 and G_2) given as:

$$GED(G_1, G_2) = \min_{G_1 \xrightarrow{d_1, \dots, d_k} G_2} \sum_{i=1}^k cost(d_i)$$

where, d_1, \dots, d_k are graph edit operations (insertion, deletion, replacement of a vertex or an edge) from G_1 to G_2 . With the exception of the abstraction split⁶, the GED for

⁶For abstraction, we observed syntax errors, e.g., missing/incorrect arguments for queries in the generated graphs like `RelationQuery(apple, slice)`, instead of `RelationQuery(apple, knife, slice)`. However, the selection of the correct query module and the partial grounding of the correct arguments lead to a significant improvement over baselines.

all test splits was observed to be ≈ 0.03 (GED \downarrow). Here, \downarrow signifies that a lower GED score is better, with the lowest value being $= 0$. Note, that although it is possible for the response to contain syntax errors, e.g., invalid names or queries with invalid arguments, the output can be improved by leveraging the DSL grammar to avoid invalid arguments.

10.2.2 Prompting Language Models

We also experimented with prompting. As a proof-of-concept, we show our example prompts in Table 10.4. We use ChatGPT [46] with few-shot prompting. The prompt is displayed in gray, the queries in blue, and the generated output in green. We observed that the use of Chain-of-Thought [66] improved the output.

10.3. Integer Programming for Alignment in NSG

The constrained optimization problem defined in Eqs. 3, without the ordering constraint, can also be formulated as an Integer Programming problem [67] where variables Z_{jt} can only take integer values in $\{0, 1\}$ (i.e. with the additional constraint $Z \in \{0, 1\}^{N \times S}$). Notably, the proposed DP solution adheres to the constraints Eqs. 3a 3b 3c. The first part of the DP (highlighted in green in Figure 4) pairs the current query q_j with the current segment s_t , then tries to align the rest of the queries with the remaining segments to meet the requirement of one query per segment, as specified in Eq. 3a. The second part of the solution (denoted by the red box) skips over the current segment s_t and tries to align the same queries with the remaining segments until a pairing is found (i.e. $Z_{jt} = 1$). Thus, together with the base case of $Z = \mathbb{I}$ if $N = S$, it satisfies Eq. 3b. Furthermore, since the DP processes the queries and segments in a specific order (topological sorting for queries and temporal order of video segments), it also meets the ordering constraint requirement specified in Eq. 3c.

10.4. NSG Analysis

- Table 6 demonstrates the robustness of NSG to changes in the window size k .
- We trained two different NSG models to compare the impact of query types with (i) `(State+Relation)Query`, (ii) `ActionQuery`. Figure 9 reveals that a combination of `(State+Relation)Query` is effective at detecting sub-tasks in segments with high recall, particularly for `slice` and `put`. We also note that the NSG model struggles to detect the `slice` sub-task in the Novel Steps split.

Table 10.4: Semantic Parsing by Prompting ChatGPT

Q. slice of apple is heated in microwave, then placed in a plate
A. First the apple is sliced, hence Step 1: slice apple. Then the apple is heated, hence Step 2: heat apple. Then the apple is placed in a plate, hence Step 3: place apple in plate. Hence, the order of the steps are: slice apple < heat apple < place apple in plate
Q. potato is cleaned in sinkbasin and sliced, then cooled in a fridge
A. First the potato is cleaned and sliced in any order, hence Step 1: clean potato; Step 2: slice potato. Then the potato is cooled in a Fridge, hence Step 3: cool potato. Hence, the order of the steps are: clean potato and slice potato < cool potato
Q. hot, sliced, clean tomato
A. First the tomato is heated and sliced and cleaned in any order, hence Step 1: heat tomato; Step 2: slice tomato; Step 3: clean tomato. Hence, the order of the steps are: heat tomato and slice tomato and clean tomato
Q. apple is heated and cleaned in sinkbasin, then cooled and sliced
A. First the apple is heated and cleaned in a sink basin in any order, hence Step 1: heat apple; Step 2: clean apple. Then the apple is cooled and sliced in any order, hence Step 3: cool apple; Step 4: slice apple. Hence, the order of the steps are: heat apple and clean apple < cool apple and slice apple.
Q. sliced apple is heated in microwave, then cleaned in a sinkbasin
A. First the apple is sliced, hence Step 1: slice apple. Then the apple is heated in a microwave, hence Step 2: heat apple. Then the apple is cleaned in a sink basin, hence Step 3: clean apple. Hence, the order of the steps are: slice apple < heat apple < clean apple
Q. apple is heated in microwave after cooling and cleaning
First the apple is cooled and cleaned in any order, hence Step 1: cool apple; Step 2: clean apple. Then the apple is heated in a microwave, hence Step 3: heat apple. Hence, the order of the steps are: cool apple and clean apple < heat apple.

- We evaluated the NSG model against the best-performing baseline (VIOLIN-ResNet) across two axes: task complexity and ordering. Figure 8 shows that NSG’s performance is robust to complexity and ordering variations.
- Since NSG only utilizes the features from aligned video segments and ignores the remaining segments, we conducted experiments to investigate the role of context (from the discarded segments) in EgoTV. Specifically, we trained an extra BiLSTM layer to encode bidirectional context from adjacent segments on top of the CLIP segment features. From Table 6, we observed improved performance across all splits, except for Novel Tasks. We attribute this to a potential loss of compositional and temporal comprehension of the segment features caused by the inclusion of additional context information.

10.5. NSG on Real-world Data

NSG for CTV. In Section 5.1, we described two symbolic operations to process task description. In CTV, all of the

NSG	Novel Tasks	Novel Steps	Novel Scenes	Abstraction
$k = 12$	90.6	50.3	81.3	82.5
$k = 20$ (default)	90.0	64.7	84.9	80.4
$k = 32$	89.2	54.9	81.0	82.3
NSG-BiLSTM	73.3	70.2	90.0	87.2

Table 6. **NSG ablations.** [Block 1]: NSG with different window sizes $k = \{12, 20, 32\}$. The best-performing NSG model with $k = 20$ is reported in Table 3. [Block 2]: NSG with BiLSTM to encode additional context from neighboring segments.

action steps refer to a certain action. Hence, we apply the ActionQuery as in Table 2 to encode all action steps. In Section 5.2, we described (1) how we processed task description into a graph and (2) how we generated all possible sequences from the graph. Since the action sequences are already given in CTV, we can skip the above two steps in Section 5.2 and directly feed the sequence in our Query Encoder and Video Aligner models.

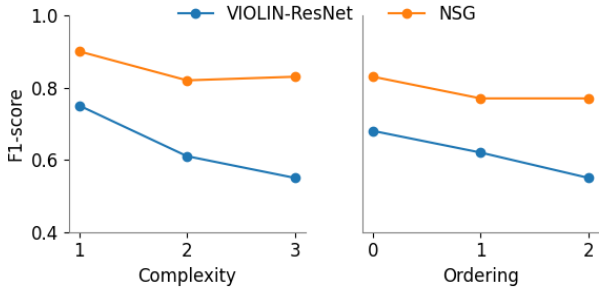


Figure 8. **NSG maintains consistent performance as task complexity and ordering difficulty increases.** F1-score of NSG vs. best-performing baseline for EgoTV tasks with varying complexity and ordering are shown.

Model	Visual	Text	Fusion	F1
VIOLIN-I3D [38]	I3D	BERT	Y	34.7
MIL-NCE [44]	S3D	Word2Vec		43.4
VideoCLIP [36]	Tx	Tx	Y	49.7
CoCa [76]	Tx	Tx	Y	70.9
NSG (ours)	CLIP	CLIP	Y	76.3

Table 7. **Performance on CTV’s test split, which mirrors the Novel Tasks split from EgoTV**

Performance Evaluation. To evaluate how NSG enables task verification in the real world, we compare the performance of NSG against selected baselines described in Sec. 6, which were either applied to the previous CrossTask evaluation (MIL-NCE[44], VideoCLIP[36]) or had competitive performance (CoCa[76], VIOLIN[38]) on EgoTV. Note that the methods for CrossTask are not directly applicable to CTV since CTV focuses on task verification (predicting if the task is accomplished) instead of temporal localization (localizing action temporally). Table 7 shows that the baseline models VideoCLIP, CoCa perform better than VIOLIN on CTV as compared to EgoTV. This indicates that CTV is potentially able to better harness the gains from the large-scale VL pretraining in these models compared to EgoTV. Despite these gains, NSG outperforms the baselines by a significant margin.

11. Baseline descriptions and details

11.1. VLM Baselines

Majority of VLMs can be characterized based on their approach of extracting and fusing features from vision and text modalities. VLMs for video tasks use either a video encoder or an image encoder with temporal aggregation using sequence model, e.g., transformers [51] or LSTM [22] to obtain the video features. The vision and text encoders can be jointly trained using either a) contrastive loss that aligns both modalities in a shared latent space e.g., CLIP [50], MIL-NCE [44], b) masked token prediction losses on the

generated text [32] aka captioning loss, or c) combination of captioning and contrastive losses [76]. The vision-text features from encoders can either be fused (multimodal fusion) using attention-based mechanisms or by computing cross-modal similarity scores. We investigate 6 VLMs that span the space of these characteristics for EgoTV.

CLIP4Clip [39] uses CLIP-based [50] text and image encoders. Parameterized (e.g., LSTM-based) or non-parameterized (e.g., mean-pooling) aggregation of the resultant image features allows video representation using a single feature vector, without any explicit fusion.

CLIP Hitchhiker [3] uses a similar encoder structure as CLIP4Clip [39] and performs weighted-mean pooling of frame embeddings using text-visual similarity scores. **CoCa** [76] uses image-text (dual) encoder-decoder architecture trained using contrastive and captioning loss. The frame-level features are pooled via attentional pooling [30] to model the temporal sequence of the video and then fused with the text features for downstream tasks. **MIL-NCE** [44] learns to encode video and text into a single vector using separate encoders (S3D[71], word2vec[45]) learned from scratch using the proposed multi-instance contrastive loss.

VideoCLIP [36] is built on top of MIL-NCE [44]. It adds additional transformer layers for video and text encoders, trained using contrastive loss. The resultant embeddings can be fused together for downstream tasks. **VIOLIN** [38] uses pre-trained image/video (e.g., ResNet [19], I3D [7]) and text encoders (e.g., GloVe [48], BERT [12]) separately and fuses the resultant representations from each modality using bi-directional attention [55]. For each of the above VLMs, we freeze the pretrained feature extractors and finetune a fully-connected probe layer, along with the temporal aggregation layers where appropriate (CLIP4Clip-LSTM, VIOLIN), using EgoTV’s train split.

11.2. Text2Text Baseline Model

In this baseline, we generate video captions from ground-truth objects and sub-task labels and calculate a text similarity score (cosine similarity) between the video caption and the task description using a pretrained RoBERTa model [81] by using a manually set threshold. Videos are split into segments, with each caption containing the segment index (for temporal grounding), scene location (kitchen), (*top-k*) objects in the scene, and the activity (sub-task). Refer to Table 10 for examples. This baseline mirrors Socratic Models [79] which generalizes in zero-shot by leveraging the multimodal capabilities from several pre-trained models. For instance, the objects from each segment can be captured using open-vocabulary VLMs [35, 80, 76], while the activities for each segment can be detected using [44, 36] by zero-shot classification with text-to-video feature similarity. Similarly, a final summarized video caption for the whole video can be generated using an LLM. No

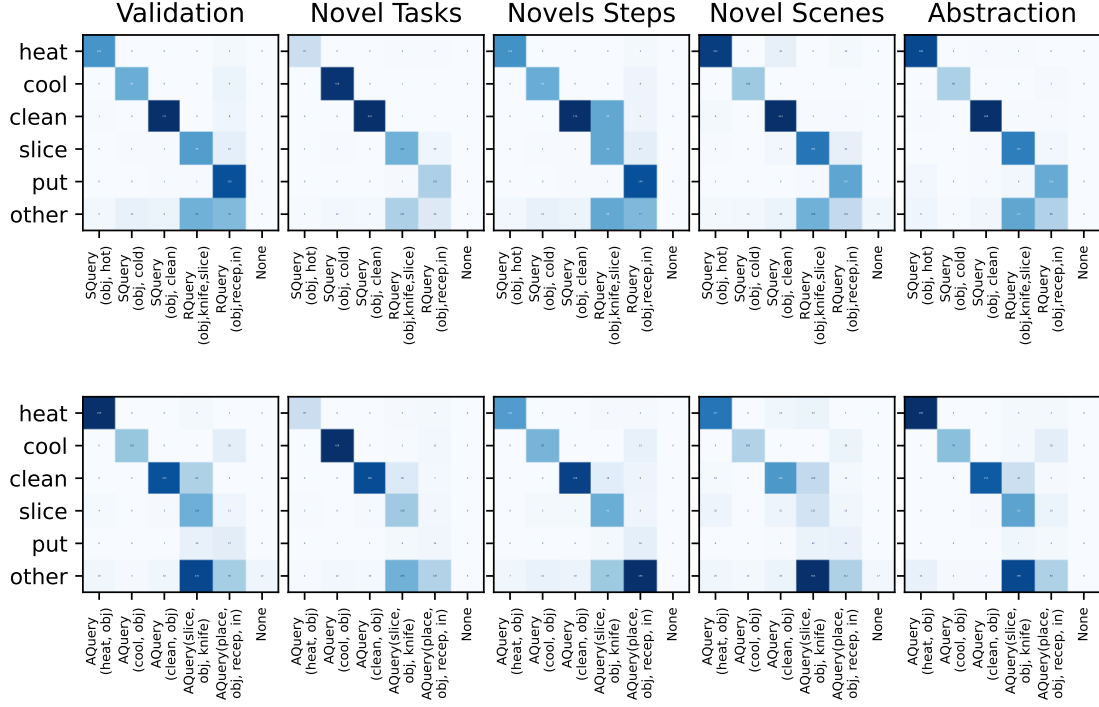


Figure 9. **Effect of query types on NSG performance.** Confusion matrices for two different query models across train/test splits of EgoTV. The Y-axis represents the ground-truth sub-task for a segment, and the X-axis denotes the aligned query for that segment. [Row 1]: Here, SQuery and RQuery denote StateQuery & RelationQuery, respectively. [Row 2]: Here, AQuery denotes ActionQuery. It can be observed that $\{\text{State+Relation}\}\text{Query}$ performs better than ActionQuery.

table, despite having ground-truth textual representations of objects and sub-tasks on a scene-by-scene basis, the Text2text baseline model fails to generalize. We attribute this to two reasons: (1) The pretrained RoBERTa model has limited capacity to capture (out-of-domain) word-level sub-task orderings to determine entailment in EgoTV, and (2) Text2Text lacks visual inputs and might suffer from lack of inferring relationships between objects.

Text2Text Baseline Examples

Text Description: apple is cooled in a Fridge and cleaned in a SinkBasin

Video Caption:

Segment: 1. Location: kitchen. Objects: countertop, apple. Activity: go to countertop
Segment: 2. Location: kitchen. Objects: fridge, apple. Activity: go to fridge
Segment: 3. Location: kitchen. Objects: apple, fridge. Activity: cool apple
Segment: 4. Location: kitchen. Objects: apple, fridge. Activity: cool apple
Segment: 5. Location: kitchen. Objects: sink, apple. Activity: go to sink
Segment: 6. Location: kitchen. Objects: apple, sink. Activity: clean apple

Task Verified: True

Text Description: lettuce is picked, cooled in a Fridge, and sliced in a SinkBasin

Video Caption:

Segment: 1. Location: kitchen. Objects: sink, lettuce. Activity: go to sink
Segment: 2. Location: kitchen. Objects: sink, lettuce. Activity: go to sink
Segment: 3. Location: kitchen. Objects: lettuce, sink. Activity: clean lettuce
Segment: 4. Location: kitchen. Objects: fridge, lettuce. Activity: go to fridge
Segment: 5. Location: kitchen. Objects: lettuce, fridge. Activity: cool lettuce

Task Verified: **False**

Figure 10. Text2Text Baseline Examples.

Complex \ Order	0	1	2
1	clean_simple, cool_simple, heat_simple pick_simple, place_simple, slice_simple		
2	clean_and_cool, clean_and_heat clean_and_place, clean_and_slice cool_and_place, heat_and_place slice_and_cool, slice_and_heat slice_and_place	clean_then_cool, clean_then_heat clean_then_place, clean_then_slice cool_then_clean, cool_then_place cool_then_slice, heat_then_clean heat_then_place, heat_then_slice slice_then_clean, slice_then_cool slice_then_heat, slice_then_place	
3	slice_and_clean_and_place, cool_and_clean_and_place cool_and_slice_and_place, heat_and_clean_and_place slice_and_heat_and_place, slice_and_heat_and_clean cool_and_slice_and_clean		clean_then_cool_then_place, clean_then_cool_then_slice clean_then_heat_then_place, clean_then_heat_then_slice clean_then_slice_then_cool, clean_then_slice_then_heat cool_then_clean_then_place, cool_then_clean_then_slice cool_then_slice_then_clean, heat_then_clean_then_place heat_then_clean_then_slice, heat_then_slice_then_clean slice_then_clean_then_place, slice_then_clean_then_heat slice_then_clean_then_clean, slice_then_clean_then_clean slice_then_cool_then_place, slice_then_heat_then_clean slice_then_heat_then_place, clean_and_cool_then_place clean_and_cool_then_slice, clean_and_heat_then_place clean_and_heat_then_slice, clean_and_slice_then_cool clean_and_slice_then_heat, clean_then_cool_and_slice clean_then_heat_and_slice, cool_and_slice_then_clean cool_then_clean_and_slice, heat_and_slice_then_clean heat_then_clean_and_slice, slice_and_clean_then_place slice_and_cool_then_place, slice_and_heat_then_place slice_then_clean_and_cool, slice_then_clean_and_heat clean_then_cool_and_place, clean_then_heat_and_place clean_then_slice_and_place, slice_then_cool_and_place slice_then_heat_and_place, slice_then_clean_and_place heat_then_clean_and_place, heat_then_slice_and_place cool_then_clean_and_place, cool_then_slice_and_place

Table 8. **List of tasks in EgoTV dataset** arranged according to complexity (rows) and ordering (columns) in the tasks. A total of 82 tasks were considered for the dataset generation, split into train and novel composition sets. **Blue** denotes novel composition tasks.

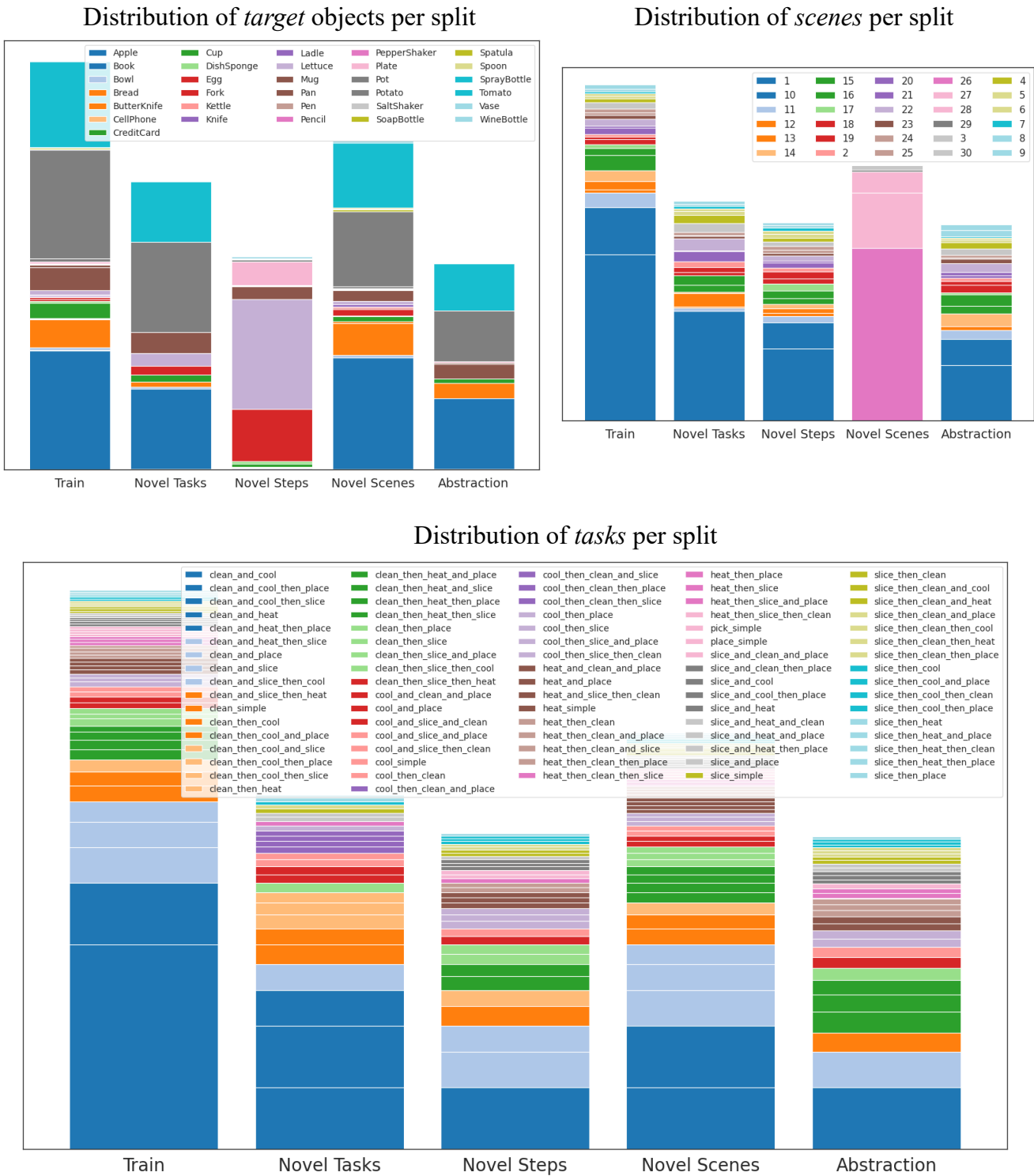


Figure 11. EgoTV dataset analysis. Distribution of *target* objects [row 1, left], *kitchen-scenes* [row 1, right], and *sub-tasks* [row 2] in each split. The Y-axis is in the log scale.